Electronic Supplementary Material (ESI) for Journal of Materials Chemistry A.

Unraveling the structure-sensitivity in N_2O photocatalytic decomposition on CeO_2: A DFT+U study

Weiyu Song[1], Lu Wang[1], Yang Gao, Jianlin Deng, Meizan Jing, Huiling Zheng Jian Liu[*], Zhen Zhao, Manglai Gao, Yuechang Wei

State Key Laboratory of Heavy Oil Processing, College of Science, China University of Petroleum-Beijing, Beijing 102249, P. R. China

[*] Corresponding author
E-mail addresses: liujian@cup.edu.cn
[1] The both authors contribute equally to this paper

1. Supplementary computational details of the relative level of CBM (Conduction Band Minimum) for (110) surface and (111) surface.

We calculated the local potential along the z-axis of the (110) surface and (111) surface which are shown in Figure S1 and Figure S2. We selected a point deep in the vacuum (13 Å) as the reference energy for (110) surface and (111) surface. In this point, the local potential are 5.41 eV and 6.37 eV, respectively. The difference of electrostatic potential is -0.96 eV. The original CBM for (110) surface and (111) surface are 0.91 eV and -0.85 eV, respectively. Therefore, the CBM for (110) surface is 2.72 eV higher than that for (111) surface.

2 Supplementary computational details of crystal orbital Hamiltonian population (COHP)

The bonding analysis have been performed through the use of the crystal orbital Hamiltonian population (COHP)[1,2] by the Lobster code. [3,4] The COHP can measure the magnitude and sign of the bond order energy overlap between atomic orbitals located on different atoms. It can determine the bonding or the antibonding nature of orbital fragments. It can also measure the interaction strength between two atomic orbitals.

References

1 R. Dronskowski and P. E. Blöchl, *J. Phys. Chem.*,1993, **97**, 8617–8624.

2 V. L. Deringer, A. L. Tchougréeff and R.Dronskowski, *J. Phys. Chem. A*, 2011, **115**, 5461–5466.

3 S. Maintz, V. L. Deringer, A. L. Tchougréeff and R. Dronskowski, *J. Comput.Chem.*, 2013, **34**, 2557–2567.

4 S. Maintz, V. L. Deringer, A. L.Tchougréeff and R. Dronskowski, *J. Comput. Chem.* 2016, **37**, 1030–1035.

Supplementary Figures

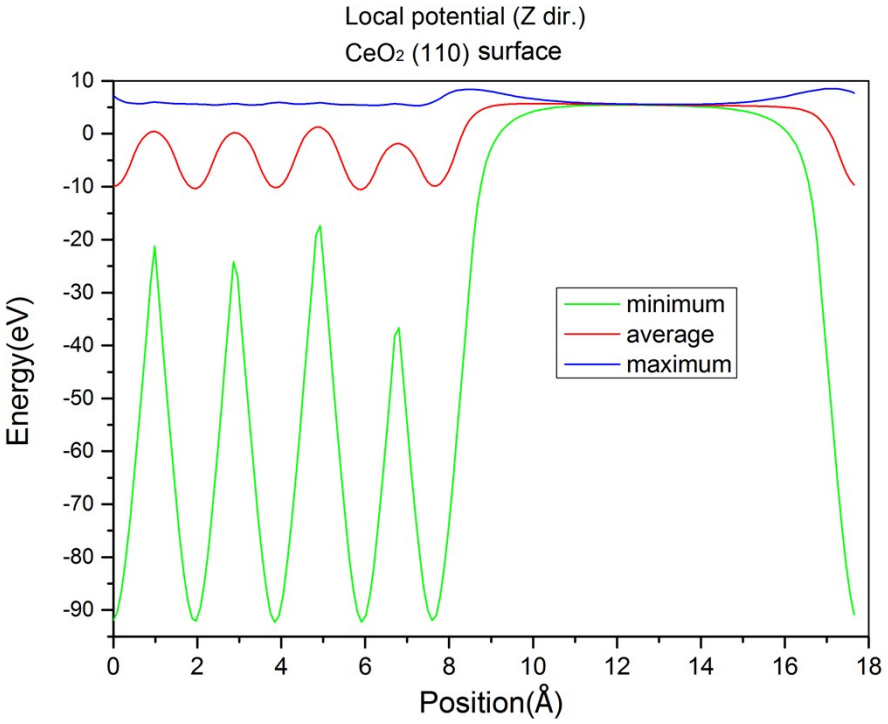

Fig. S1 The local potential along the z-axis of the (110) surface

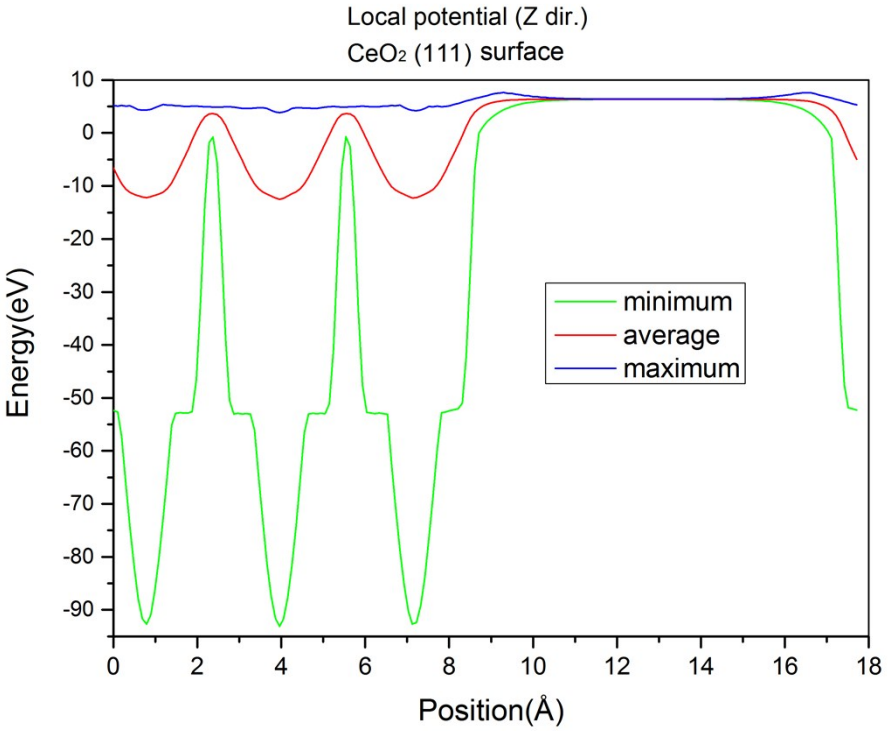

Fig. S2 The local potential along the z-axis of the (111) surface

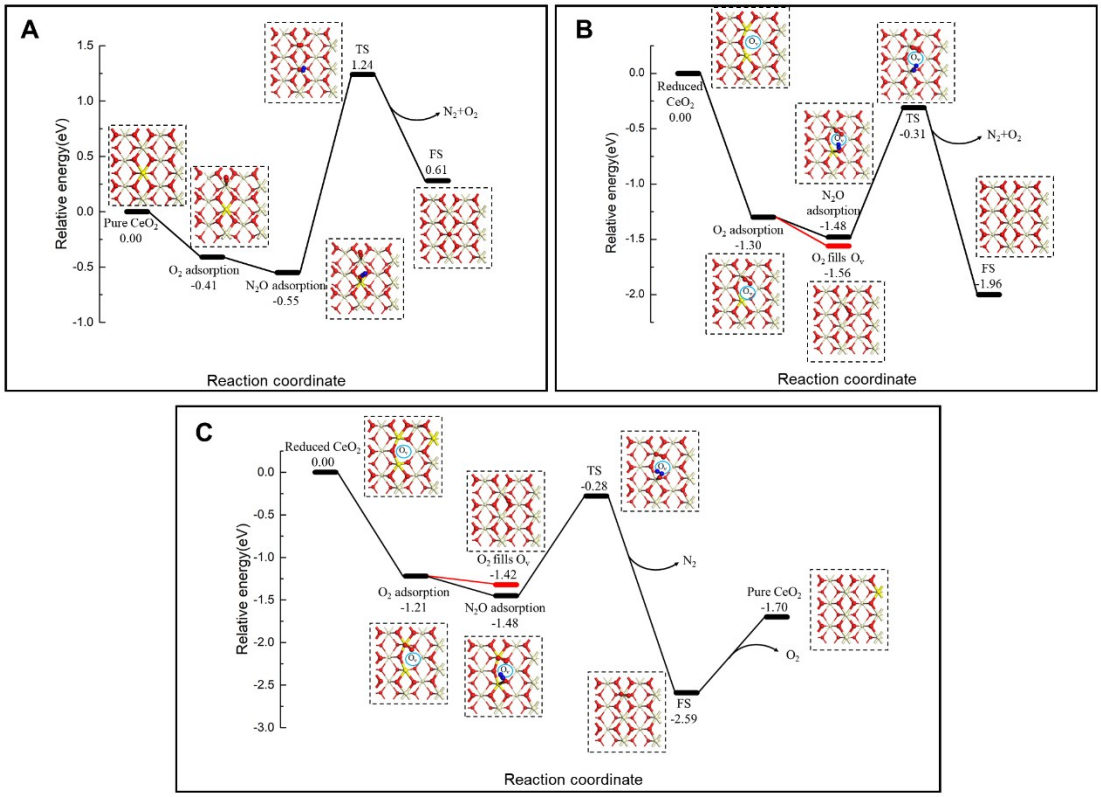

Fig. S3 Relative energy diagram for the reaction of N_2O decomposition in the presence of O_2 on the pure (A) and reduced CeO_2 (110) surface with(C) and without(B) the excited electron.

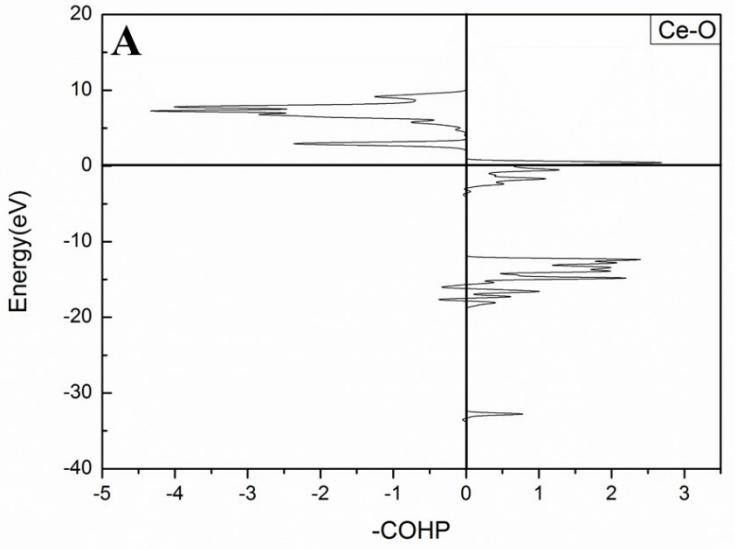
A
Ce-O
Energy(eV)
-COHP

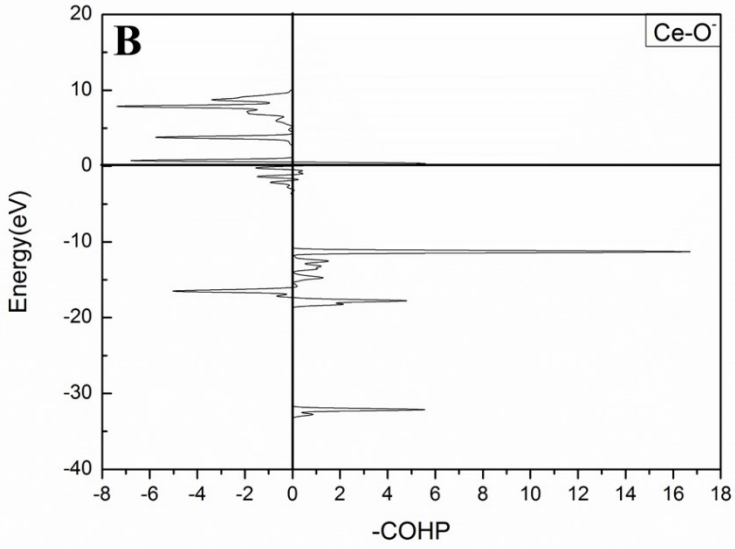
B
Ce-O-
Energy(eV)
-COHP

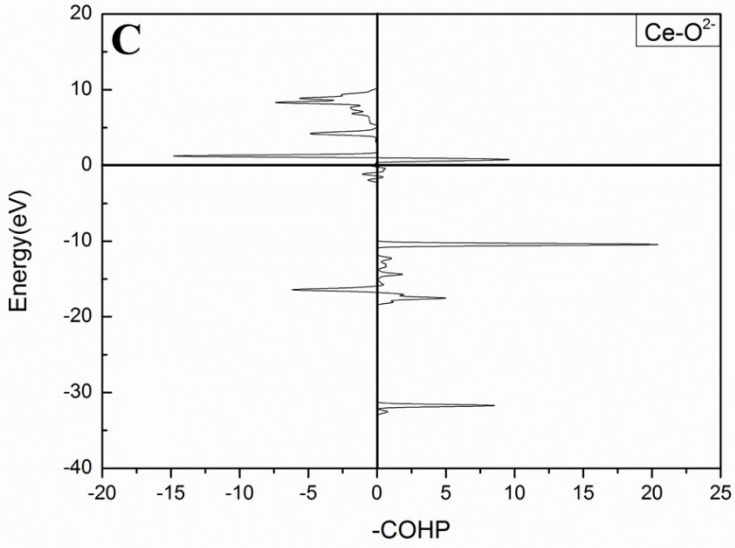
C
Ce-O2-
Energy(eV)
-COHP

Fig. S4 -COHP between Ce and O as the state of O(A), O^{-}(B) and O^{2-}(C) for (110) surface. Fermi level is set to zero.

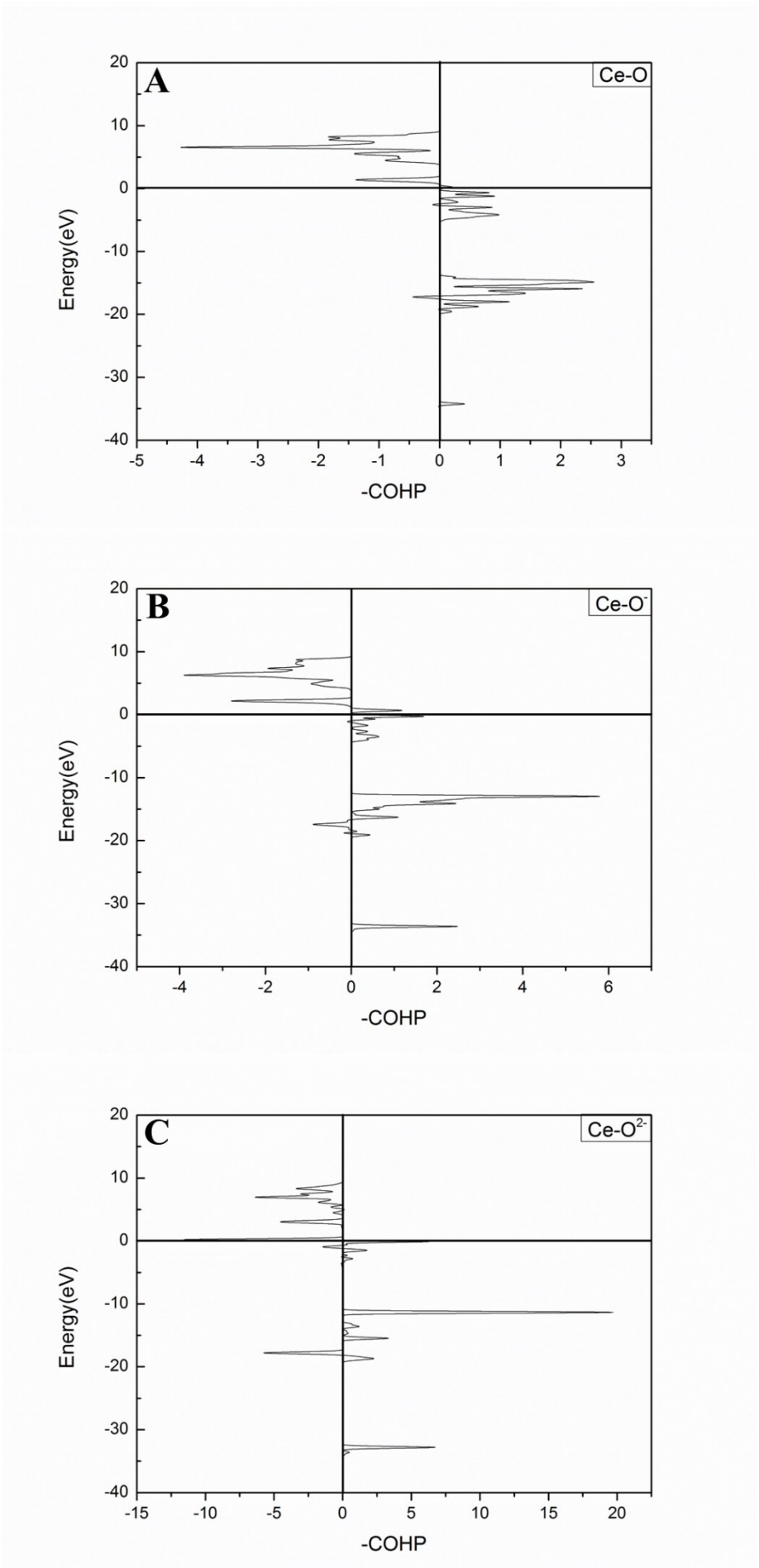
A
Ce-O
Energy(eV)
-COHP
B
Ce-O-
Energy(eV)
-COHP
C
Ce-O2-
Energy(eV)
-COHP

Fig. S5 -COHP between Ce and O as the state of O(A), O^{-}(B) and O^{2-}(C) for (111) surface. Fermi level is set to zero.

Table S1 The vibrational frequencies for all transition states

Surface		Reaction	Transition state	Vibrational frequencies/ cm^{-1}	Corresponding figure
110 surface	Clean	Thermocatalysis	N-O bond cleavage	676.99	Fig. 6(A)
		Photocatalysis	N-O bond cleavage	332.39	Fig. 6(B)
		Photocatalysis	O-O bond coupling	508.52	Fig. 7(A)
		Thermocatalysis	O-O bond coupling	239.29	Fig. 7(B)
	Reduced	Thermocatalysis	N-O bond cleavage	533.77	Fig. 8(A)
		Photocatalysis	N-O bond cleavage	583.34	Fig. 8(B)
111 surface	Clean	Thermocatalysis	N-O bond cleavage	554.34	Fig. 9(A)
		Photocatalysis	N-O bond cleavage	392.87	Fig. 9(B)
	Reduced	Thermocatalysis	N-O bond cleavage	347.92	Fig. 10(A)
		Photocatalysis	N-O bond cleavage	418.08	Fig. 10(B)